Journal of Materials Science and Chemical Engineering, 2022, 10, 1-12
https://www.scirp.org/journal/msce
ISSN Online: 2327-6053
ISSN Print: 2327-6045

Effect of Ultrasound on the Pseudoelasticity of Shape Memory Alloys

Ali H. Alhilfi[1], Andrew Rusinko[2]

[1]Misan University, Misan, Iraq
[2]Obuda University, Budapest, Hungary
Email: alihameed@stud.uni-obuda.hu, ruszinko.endre@uni-obuda.hu

How to cite this paper: Alhilfi, A.H. and Rusinko, A. (2022) Effect of Ultrasound on the Pseudoelasticity of Shape Memory Alloys. *Journal of Materials Science and Chemical Engineering*, **10**, 1-12.
https://doi.org/10.4236/msce.2022.106001

Received: April 21, 2022
Accepted: June 12, 2022
Published: June 15, 2022

Abstract

The paper aims to develop a model describing the ultrasound-assisted pseudoelastic deformation of shape memory alloys. Experimental results record that acoustic energy reduces the value of stresses needed to induce pseudoelastic deformation (martensitic transformation). At the same time, the ultrasound-assisted deforming develops with a more significant strain hardening. The model presented here is based on the synthetic theory of inelastic deformation. To catch the phenomena caused by acoustic energy, we enter into the basic equation of the synthetic theory terms reflecting the effect of ultrasound on the processes governing the peculiarities of pseudoelastic deformation in the acoustic field. The analytical results fit good experimental data.

Keywords

Shape Memory Alloys, Pseudoelasticity, Martensite Transformation, Ultrasound

1. Introduction

Shape memory alloys (SMA) have been widely used in various technical applications. The superior property of SMA is that it can go through solid-state phase transformations, meaning it can be stretched, bent, heated, cooled, and still remember its original shape. SMAs are widely used for medical implants in medicine due to their kink resistance, stress constancy, high elasticity, and corrosion resistance. If we speak of electronics devices and robotic systems, SMA actuators, sensors, and controllers have drawn significant attention and interest due to their unique properties. They are expected to be equipped with many modern vehicles at competitive market prices [1]. The essential advantage is that active elements (e.g., SMA wire or spring) can be deformed by applying minimal ex-

ternal force and retain their previous form when subjected to certain stimuli such as thermomechanical or magnetic changes. In aerospace, SMA release devices can be actuated slowly, avoiding satellite shock failures. This application is essential for satellites because it can also be used for "microsatellites" since compact separation devices with minimal SMA release triggers can be made [2].

There has been a strong interest in studying direct (martensite) and reverse (austenite) transformation [3]-[8] in recent years. With strain recovery (austenite transformation) in an ultrasonic field, impulses of acoustic energy result in stepwise negative increments of the deformation [3] [4] [5] [6].

With martensite transformation in the acoustic field, this paper focuses on pseudoelastic deformation at constant temperature under the simultaneous action of static and ultrasonic stresses. Consider experimental results recorded by Steckmann *et al.* [9]. **Figure 1** shows the σ~ε diagrams in uniaxial tension of Ni-Ti-Re alloy. While line 1 demonstrates conventional, line 2 shows ultrasound-assisted pseudoelastic deformation. The following peculiarities of the pseudoelasticity coupled with ultrasound are easy to be observed:

1) The pseudoelastic deformation in the acoustic field starts at lower stress than for the static loading (compare ≈ 48 Mpa for line 2 to approximately 100 MPa for line 1), and the initial and middle portion of σ~ε diagram runs at lower values of stresses compared to line 1.

2) Line 2 has a greater slope angle than line 1 and crosses it at the deformation of about 6.3%, which means that, from this point, greater stresses are needed compared to the ordinary case.

To explain the mechanisms governing the ultrasound-assisted martensite transformation, we address the results of experimental investigations [3]-[13]:

1) Ultrasound increases the mobility of interfaces (phases and domains) by decreasing the efficient friction force caused by alternate stresses.

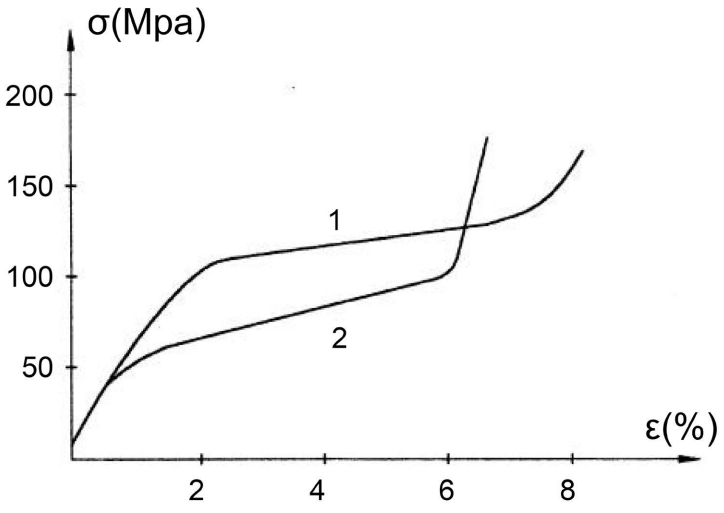

Figure 1. Pseudoelastic deformation of Ni-Ti-Re alloy, temperature 283 K; 1—without ultrasonics, 2—under superimposed ultrasonics with amplitude of ultrasonics deformation $\varepsilon_m = 2 \times 10^{-4}$ [9].

2) The superposition of alternate stresses induces the movement of defects (dislocations and twins) and martensitic domain boundaries (within the temperature range of martensitic transformation). In addition, acoustic energy results in the appearance of an additional quantity of preferably oriented domains that leads to a further strain variation.

On the other hand, Malygin's [14] and Sapozhnikov's [15] investigations show that the superimposed ultrasound can favor the increase or decrease of the static stress needed to develop the pseudoelastic deformation. This is because, at the initial stage of pseudoelastic deformation, the oscillatory stress causes the fraction of the martensite phase to increase during positive half-cycles, which leads to an additional amount of deformation and, hence, to a decrease in the applied stress. In the case of large stresses, the effect of the oscillatory stress is more significant during negative half-cycles leading to a decrease in the volume fraction of martensite and, hence, to an increase in the applied stress. Therefore, the sign of the effect of acoustic energy on the development of martensite transformation varies during pseudoelastic deformation. This result correlates with that indicated by Steckmann [9], where the ultrasound-assisted stress-strain diagram has a greater hardening coefficient and therefore crosses the ordinary diagram.

The synthetic theory of inelastic deformation is utilized to model the results shown in **Figure 1**. This theory has established itself as a reliable instrument for modeling classical problems of phase transformations [16] [17] [18].

This paper aims to extend the synthetic theory to develop a model describing the ultrasound-assisted pseudoelastic deformation of Ni-Ti-Re alloy.

2. Synthetic Theory

The synthetic theory operates with notions used in the Ilyushin deviatoric space, stress ($\boldsymbol{S}$) and strain ($\boldsymbol{e}$) vectors [17]. For a three-dimensional subspace (S^3) of the Ilyushin five-dimensional deviatoric space, their components are

$$\begin{aligned} S_1 &= \sqrt{3/2}S_{xx},\ S_2 = S_{xx}/\sqrt{2} + \sqrt{2}S_{yy},\ S_3 = \sqrt{2}S_{xz} \\ e_1 &= \sqrt{3/2}e_{xx},\ e_2 = e_{xx}/\sqrt{2} + \sqrt{2}e_{yy},\ e_3 = \sqrt{2}e_{xz} \end{aligned} \tag{1}$$

where S_{ij} and e_{ij} are the stress and strain deviator tensor components, respectively. As a two-level model, the synthetic theory calculates the macroscopic deformation as an averaging (summation) of deformations occurring on the microlevel of material. For the macro level, we take the elementary volume of the body, which is considered as a point in the mathematical sense. This volume consists of a large number of micro volumes, each being an element of the continuum, capable of deforming under external effects. Thus, macrodeformation is defined as the integration (summation) of deformations occurring on the microscopic level of material. As a result, we propose the following formula for strain vector components (e_i):

$$e_k = \iiint_V \varphi_N N_k \mathrm{d}V,\ k = 1,2,3. \tag{2}$$

In Equation (2), φ_N is named strain intensity; it is an average measure of

deformation within one element of microstructure. A unit vector $\boldsymbol{N}$ gives the orientation of this element, its components N_k are defined via spherical angles α, β, and λ as [17]

$$N_1 = \cos\alpha\cos\beta\cos\lambda,\ N_2 = \sin\alpha\cos\beta\cos\lambda,\ N_3 = \sin\beta\cos\lambda. \tag{3}$$

The whole range of angles α, β, and λ is $0 \le \alpha \le 2\pi$, $0 \le \beta \le \pi/2$, and $0 \le \lambda \le \pi/2$. Finally, $\mathrm{d}V$ from (2) is an elementary set of micro volumes involved in the deformation, $\mathrm{d}V = \cos\beta \mathrm{d}\alpha\mathrm{d}\beta$ [17].

Now, we must define the strain intensity. To apply Equation (2) to the description of deformation induced by phase transformations, we relate the strain intensity rate to the rate of martensite fraction ($\dot{\Phi}$):

$$r\dot{\phi}_N = \dot{\Phi}, \tag{4}$$

where r is the model constant that reflects the strain hardening of the material, *i.e.*, it governs the slope of σ~ε curve [17]. We define $\dot{\Phi}$ for direct (martensitic) transformation as (**Figure 2**)

$$\dot{\Phi} = -\frac{\dot{T}_e}{M_s - M_f}, \tag{5}$$

where M_s and M_f are the material constants symbolizing the start and finish temperatures of martensite transformation. This formula holds at

$$\dot{T}_e < 0 \text{ and } M_f < T_e < M_s \tag{6}$$

In the above formulae, T_e is effective temperature whose definition has been proposed in terms of the structural-analytic model developed by Lihachev and Malinin [19] through the Clausius-Clapeyron equation as:

$$T_e = T\left(1 - D\boldsymbol{S}\cdot\boldsymbol{N}\right). \tag{7}$$

Equation (7) enables one to account for the shift of the characteristic temperatures caused by loading. Summarizing the above-mentioned, formulae (5)-(7) define the amount of martensite as a single-valued function of temperature and acting load. The scalar product $\boldsymbol{S}\cdot\boldsymbol{N}$ gives the resolved shear stress acting in the element with $\boldsymbol{N}$-orientation. This product reflects the well-known fact that external load manifests itself differently depending on how preferable the element's/slip system's orientation is.

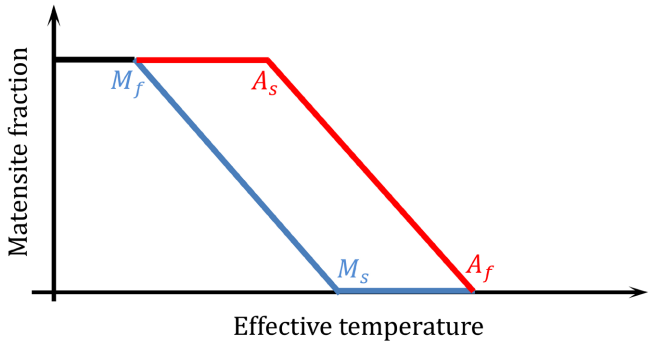

Figure 2. Φ~T_e plot.

With Equations (4), (5), and (7), φ_N is

$$r\dot{\varphi}_N = \dot{\Phi} = -\frac{\dot{T}_e}{M_s - M_f}. \tag{8}$$

Considering that $\varphi_N = \Phi = 0$ as $T_e = M_s$, we get

$$\Phi = \frac{M_s - T_e}{M_s - M_f}. \tag{9}$$

or

$$r\varphi_N = M_s - T_e. \tag{10}$$

In the formula (10), the constant r includes $M_s - M_f$.

Let us apply Equations (7) and (10) for the case of iso-thermal uniaxial tension ( ) when the stress vector, according to (1), has only one non-zero component, $S_1 = \sqrt{2/3}\sigma \equiv S$. Together with (3), we have

$$T_e = T_0\left(1 - DS\sin\beta\cos\lambda\right). \tag{11}$$

$$r\varphi_N = M_s - T_0\left(1 - DS\sin\beta\cos\lambda\right). \tag{12}$$

First, derive a formula for the first value of tensile stress (S_Φ) inducing martensitic transformation in the material. Equating the minimum value of T_e from (11) – $\beta = \pi/2$ and $\lambda = 0$ – to M_s, we obtain

$$S_\Phi = \frac{1}{D}\left(1 - \frac{M_s}{T_0}\right). \tag{13}$$

The range of the angles β and λ giving positive values for φ_N are

$$\beta_1 \le \beta \le \pi/2 \text{ and } 0 \le \lambda \le \lambda_1, \tag{14}$$

where λ_1 and β_1 are calculated from conditions $\varphi_N = 0$ and $\lambda = 0$, respectively [17]:

$$\cos\lambda_1 = \frac{1}{DS\sin\beta}\left(1 - \frac{M_s}{T_0}\right), \quad \sin\beta_1 = \frac{1}{DS}\left(1 - \frac{M_s}{T_0}\right) \tag{15}$$

Outside the range (14), we set $\varphi_N = 0$.

Substituting the strain intensity φ_N from formula (12) to Equation (2), we get the pseudoelastic strain component in uniaxial tension ($e_1 \equiv e$) as

$$e = \frac{2\pi}{r}\int_0^{\pi/2}\int_0^{\pi/2}\left[M_s - T_0\left(1 - DS\sin\beta\cos\lambda\right)\right]\sin\beta\cos\lambda\cos\beta\mathrm{d}\beta\mathrm{d}\lambda. \tag{16}$$

The factor 2π stands here because Equation (12) does not contain angle α for uniaxial tension.

Figure 3 explains what angles give positive values of the strain intensity during the integrating by formula (16). In the initial stages of transformation (**Figure 3(a)**), the integration is conducted on the angle range determined via Equations (14) and (15) as

$$e = \frac{2\pi}{r}\int_0^{\lambda_1}\int_{\beta_1}^{\pi/2}\left[M_s - T_0\left(1 - DS\sin\beta\cos\lambda\right)\right]\sin\beta\cos\lambda\cos\beta\mathrm{d}\beta\mathrm{d}\lambda. \tag{17}$$

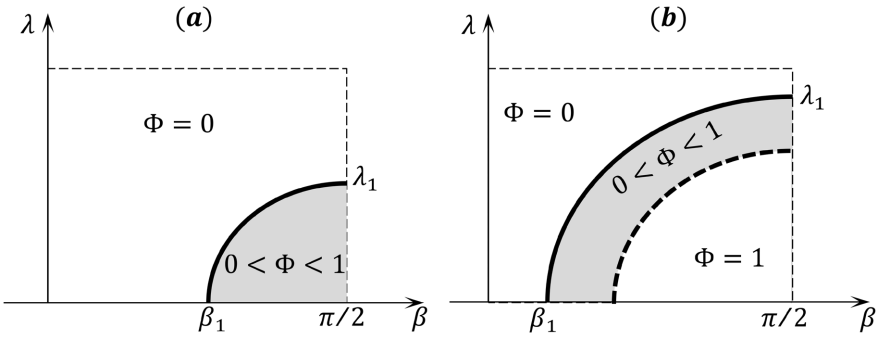

Figure 3. Development of martensite transformation in the angle coordinates.

At the same time, as Φ becomes equal to 1 for given microvolumes, the further development of martensite trans-formation terminates, and there is no further increment in the deformation for these directions (Figure 3(b), domain $\Phi = 1$). When the condition $\Phi = 1$ extends to the whole range of angles – $0 \le \beta \le \pi/2$, and $0 \le \lambda \le \pi/2$ – we obtain a fully martensitic state of the material. The further increase in the loading will result in elastic deformation only. The first moment (stress S_f) when the condition $\Phi = 1$ fulfills is calculated from Equation (11) by letting $T_e = M_f$ at $\beta = \pi/2$ and $\lambda = 0$:

$$S_f = \frac{1}{D}\left(1 - \frac{M_f}{T_0}\right). \tag{18}$$

The stress S_f symbolizes the inflection point on the σ~ε diagram from concave to convex portion.

3. Extension of the Synthetic Theory to the Ultrasound-Assisted Pseudoelasticity

Since effective temperature is the most crucial factor in the progress of phase transformation – T_e directly influences the values of Φ and φ_N –, we propose to extent Equation (7) by a term reflecting the presence of ultra-sound. Following the observations on the effect of acoustic energy on martensitic transformation, we propose to shift (decrease) the value of effective temperature by a term (U) representing the ultrasound action:

$$T_e = T_0\left(1 - D\boldsymbol{S}\cdot\boldsymbol{N} + U\right). \tag{19}$$

We define U as

$$U = U_1\left(\boldsymbol{S}_U \cdot \boldsymbol{N}\right), \tag{20}$$

where U_1 is a model constant; $\boldsymbol{S}_U$ is a stress vector whose components are formed via Equation (1) by the values of alternating stress amplitudes. The scalar product ($\boldsymbol{S}_U \cdot \boldsymbol{N}$) in formula (20) expresses the well-known fact that the effectiveness of ultrasound depends on the orientation of the microregion considered.

The term U inserted into Equation (19) represents only an assisting effect of ultrasound upon the pseudoelasticity.

On the other hand, acoustic energy can decrease or increase the stress to be applied and increase the slope angle of the stress-strain curve. To account for this, we increase the value of the constant r, which is responsible for the slope angle of the stress-strain diagram, by $U_2\left|\boldsymbol{S}_U\right|$. As a result, the ultrasound-assisted diagram inevitably crosses the ordinary one, which symbolizes that the pseudoelastic deformation needs greater stresses starting from this point. A new constant, r_U, is related to r as

$$r_U = r + U_2\left|\boldsymbol{S}_U\right|, \tag{21}$$

where U_2 is a model constant. Formula (21) is in line with the increase in the hardening coefficient proposed in [7].

It is easy to see that as $\boldsymbol{S}_U = 0$, *i.e.*, in the absence of ultrasound, we arrive at the relationships to be applied to the modeling of ordinary pseudoelastic $\sigma\sim\varepsilon$ diagrams.

Consider a material in an austenitic state ($\Phi = 0$). Taking temperature constant (T_0), we load the material by the simultaneous action of uniaxial tension and longitudinal vibration. In this case, according to Equation (1), the vector $\boldsymbol{S}_U$, has components ($\sqrt{2/3}\sigma_m, 0, 0$), where σ_m is the amplitude of oscillating tension-compression stress.

According to Equations (10) and (19)-(21), the strain intensity with superimposed ultrasound (φ_{NU}) is

$$r_U\varphi_{NU} = M_s - T_0\left[1-\left(DS + U_1S_m\right)\sin\beta\cos\lambda\right]. \tag{22}$$

Now the pseudoelastic deformation starts as

$$S_{\Phi U} = \frac{1}{D}\left[1-\left(\frac{M_s}{T_0}+U_1S_m\right)\right]. \tag{23}$$

The above formula is obtained from Equation (22) via condition $T_e = M_s$, which is the same as $\varphi_{NU} = 0$, at $\beta = \pi/2$ and $\lambda = 0$.

Formula (23) testifies – $S_{\Phi U} < S_\Phi$ – that the superposition of ultrasound lowers the value of static stress needed to induce martensite transformation/pseudoelastic deformation.

The pseudoelastic strain component (e_U), according to Equations (2) and (22), takes the following form in the presence of ultrasound

$$e_U = \frac{\pi}{r_U}\int_0^{\pi/2}\int_0^{\pi/2}\left[M_s - T_0\left[1-\left(DS+U_1S_m\right)\sin\beta\cos\lambda\right]\right]\sin 2\beta\cos\lambda\,\mathrm{d}\beta\,\mathrm{d}\lambda\,. \tag{24}$$

The boundary angles in formula (24) are

$$\cos\lambda_{1U} = \frac{1}{\left(DS+U_1S_m\right)\sin\beta}\left(1-\frac{M_s}{T_0}\right),\ \sin\beta_{1U} = \frac{1}{DS+U_1S_m}\left(1-\frac{M_s}{T_0}\right). \tag{25}$$

Let us calculate the stress value when the σ~ε diagram has a reflection point (S_{fU}) in the acoustic field. To do this, we equate T_{eU} from formula (19) at $\beta = \pi/2$ and $\lambda = 0$ to M_f. As a result:

$$S_{fU} = \frac{1}{D}\left(1 - \frac{M_f}{T_0} - U\right) < S_f . \quad (26)$$

The inequality $S_{fU} < S_f$ correctly reflects the experimental result (Figure 1) that the ultrasound-assisted pseudoelasticity tends to its completion at a smaller deformation value than that in the ultrasound-free case.

And lastly, the constant r_U that stands in formula (24) reflects another experimental fact that the sign of the ultra-sonic action changes from positive (assisting) to negative (suppressing) depending on the stage of transformation. The inequality $r_U > r$ ensures that closer to the finish of the transformation, the ultrasound-assisted σ~ε diagram runs above the ordinary one.

Therefore, the extension of the synthetic theory expressed in formulae (19)-(26) leads to a qualitative correspondence with experiments. The next step is to inspect its quantitative correctness.

4. Results. Discussion

Here, our goal is to plot σ~ε diagrams of NiTiRe alloy at a constant temperature $T_0 = 283$ K in an acoustic field. The samples at austenite state were loaded in uniaxial tension within the martensite transformation temperature range. Two loading regimes were applied: 1) static stress alone and 2) static and vibrating stresses. The amplitude of ultrasonic deformation was $\varepsilon_m = 2\times10^{-4}$ [9]. The amplitude of alternating stress is

$$\sigma_m = E\varepsilon_m , \quad (27)$$

where E is the Young modulus, $E = 80$ GPa. As a result, we obtain $\sigma_m = 16$ MPa.

First, we plot σ~ε diagram without ultrasonic action (Figure 4, line 1). To do this, we use Equations (13)-(18). As a result, we arrive at the correct results: 1) $S_\Phi = 88.3$ MPa and 2) the model $\sigma\sim\varepsilon$ curve shows good agreement with the experiment (Figure 4). Line 1 in Figure 4 is constructed with the following values of constants: $D = 1.2\times10^{-4}$ MPa^{-1}, $r = 1300$ K, $M_s = 280$ K, $M_f = 260$ K.

The next step is σ~ε diagram at the presence of ultrasound (line 2 in Figure 4). The model results have been obtained via formulae (19)-(25) with the following values of constants: $U_1 = 3.75\times10^{-2}$ MPa^{-1}, $U_2 = 22$ K/MPa. It must be stressed that the values of constants D and r remain unchangeable.

Inspect the behavior of the strain intensity for variously oriented microvolumes for ordinary and ultra-sound-assisted deformations. Figure 5 demonstrates $\varphi_{NU} \sim \sigma$ and $\varphi_N \sim \sigma$ plots obtained via Equations (22) and (12), respectively.

The following conclusion can be derived from this figure:

1) According to Equation (23), the start of ultrasound-assisted plastic (pseudoelastic) deformation takes place at $S_{\Phi U} = 38.3$ MPa (compare to $S_\Phi = 88.3$ MPa without ultrasound).

2) The stress range where pseudoelastic deformation develops is shifted toward smaller stresses.

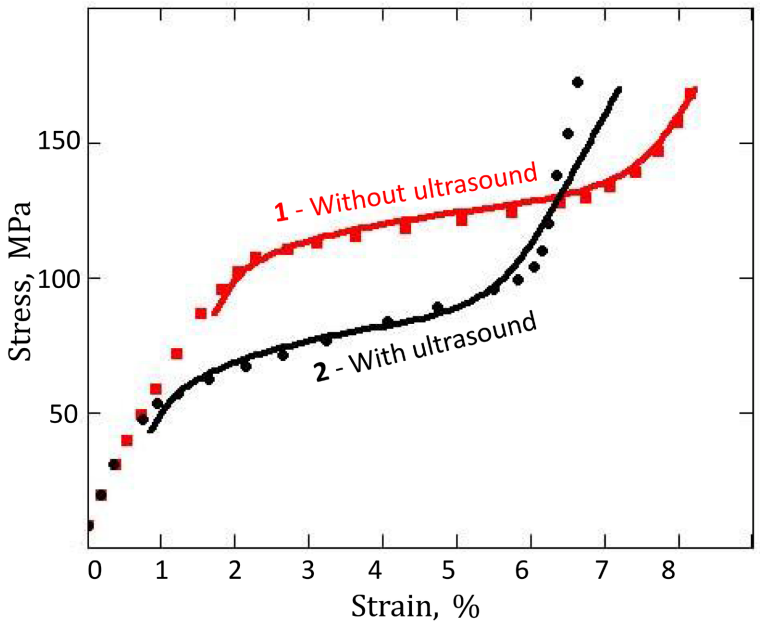

Figure 4. Pseudoelastic σ~ε diagram of NiTiRe alloy at constant temperature (T_0 = 283 K) in uniaxial tension: 1—static loading, 2—simultaneous action of static and ultrasonic loading (f = 18 kHz). Lines—model, symbols—experiment [9].

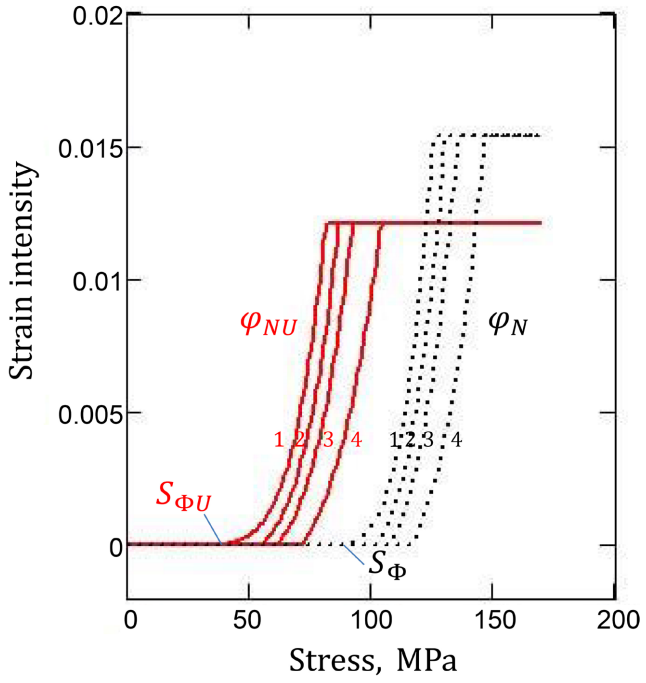

Figure 5. Strain intensity Vs. Stress plots for various directions 1 - 4: $\beta = \pi/2, \pi/4, \pi/6, \pi/12$ ($\lambda = 0$)

The above-listed points have been achieved by introducing the term U into the formula for the effective temperature.

With r_U from Equation (21) standing in the denominator in formula (24), we have obtained the result correlating with Malygin's predictions [14], namely:

3) Acoustic energy can decrease or increase the stresses needed to develop pseudoelastic deformation (in our case, the sign of ultrasonic action changes at the very end of the transformation, $\varepsilon \approx 6.4\%$).

All the results above are in full accordance with the experimental records. Therefore, we may conclude that the extension of the synthetic theory leads to qualitatively and quantitatively correct results.

5. Conclusions

We developed a model that predicts the kinetics of ultrasound-assisted pseudoelastic deformation. This model was created in terms of the synthetic theory of inelastic deformation. Following the results of experimental observations, stating that the presence of ultrasound lowers the stress needed to start martensite transformation, we extended the formula for effective temperature by a term accounting for the presence of acoustic energy. This term reflects experimentally recorded facts that acoustic energy increases the mobility of interfaces (phases and domains) and induces the movement of crystalline lattice defects (dislocations, twins, etc.). At the same time, the effect of ultrasound on stress is not monotonic during the pseudoelastic deforming. Closer to the finish of the transformation, greater stress is needed. To catch this phenomenon, we increased the factor governing the slope of the stress-strain diagram by the amplitude of vibrating stress. As a result, the ultrasound-assisted stress-strain diagram runs above the ordinary one at high stresses.

Therefore, the following results have been achieved:

1) We derived a formula that enables us to plot a stress-strain diagram under the simultaneous action of static and alternating stresses.

2) We calculated the stresses needed to start/finish martensite transformation in the acoustic field.

Acknowledgements

This work is supported by Doctoral School of Materials Sciences and Technologies, Obuda University (215-2017/6/IX/16/2/), Hungary.

Conflicts of Interest

The authors declare no conflicts of interest regarding the publication of this paper.

References

[1] Jani, J.M., Leary, M. and Subic, A. (2014) Shape Memory Alloys in Automotive Applications. *Applied Mechanics and Materials*, **663**, 248-253. https://doi.org/10.4028/www.scientific.net/AMM.663.248

[2] Wanhill, R.J.H. and Ashok, B. (2017) Shape Memory Alloys (SMAs) for Aerospace Applications. In: Prasad, N. and Wanhill, R., Eds., *Aerospace Materials and Material Technologies*, Springer, Singapore, 467-481. https://doi.org/10.1007/978-981-10-2134-3_21

[3] Rubanik Jr., V.V., Rubanik, V.V. and Klubovich, V.V. (2003) The Ultrasounds Initiation of Shape Memory Effect. *Journal de Physique IV* (*Proceedings*), **112**, 249-251. https://doi.org/10.1051/jp4:2003876

[4] Rubanik Jr., V.V., Rubanik, V.V. and Klubovich, V.V. (2008) The Influence of Ultrasound on the Shape Memory Behavior. *Materials Science and Engineering A*, **481-482**, 620-622. https://doi.org/10.1016/j.msea.2007.02.134

[5] Bao, M., Zhou, Q., Dong, W., Lou, X. and Zhang, Y. (2013) Ultrasound-Modulated Shape Memory and Payload Release Effects in a Biodegradable Cylindrical Rod Made of Chitosan-Functionalized PLGA Microsphere. *Biomacromolecules*, **14**, 1971-1979. https://doi.org/10.1021/bm4003464

[6] Breczko, T.M. and Rubanik, V.V. (1999) Study of Behaviour NiTi Alloy under Action of Ultrasound. *Proceedings of SPIE, Nondestructive Testing and Computer Simulations in Science and Engineering*, **3687**, 310-312. https://doi.org/10.1117/12.347443

[7] Sathish, S., Mallik, U. and Raju, T. (2013) Corrosion Behavior of Cu-Zn-Ni Shape Memory Alloys. *Journal of Minerals and Materials Characterization and Engineering*, **1**, 49-54. https://doi.org/10.4236/jmmce.2013.12010

[8] Desai, N.S.V., Basavarajappa, S., Arun, K. and Yadav, S. (2010) Hot Rolling and Ageing Effect on the Pseudoelasticity Behaviour of Ti-Rich TiNi Shape Memory Alloy. *Journal of Minerals and Materials Characterization and Engineering*, **9**, 343-351. https://doi.org/10.4236/jmmce.2010.94025

[9] Steckmann, H., Kolomytsev, V.I. and Kozlov, A.V. (1999) Acoustoplastic Effect in the Shape Memory Alloy Ni-Ti-Re at Ultrasonic Frequency. *Ultrasonics*, **37**, 69-62. https://doi.org/10.1016/S0041-624X(98)00031-6

[10] Belyaev, S., Volkov, A. and Resnina, N. (2014) Alternate Stresses and Temperature Variation as Factors of Influence of Ultrasonic Vibration on Mechanical and Functional Properties of Shape Memory Alloys. *Ultrasonics*, **54**, 84-89. https://doi.org/10.1016/j.ultras.2013.06.010

[11] Buchelnikov, V., Pikshtein, I., Grechishin, R., Khudoverdyan, T., Koledov, V., Kuzavko, Y., Nazarkin, I., Shavrov, V. and Takagi, T. (2004) Ultrasound-Induced Martensitic Transition in Ferromagnetic $Ni_{2.15}Mn_{0.81}Fe_{0.04}Ga$ Shape Memory Alloy. *Journal of Magnetism and Magnetic Materials*, **272**, 2025-2026. https://doi.org/10.1016/j.jmmm.2003.12.778

[12] Klubovich, V.V., Rubanik, V.V., Likhachev, V.A., Rubanik Jr, V.V. and Dorodeiko, V.G. (1997) Generation of Shape Memory Effect in TiNi Alloy by Means of Ultrasound. *Proceedings of the* 2*nd International Conference on Shape Memory and Superelastic Technologies* (*SMST*-97), California, 59-64.

[13] Samigullina, A., Murzinova, M., Mukhametgalina, A., Zhilyaev, A.P. and Nazarov, A. A. (2018) Effect of Ultrasonic Treatment on the Characteristics of Superplasticity of Titanium Alloy Ti-6Al-4V. *Defect and Diffusion Forum*, **385**, 53-58. https://doi.org/10.4028/www.scientific.net/DDF.385.53

[14] Malygin, G.A. (2001) Diffuse Martensitic Transitions and the Plasticity of Crystals with a Shape Memory Effect. *Physics-Uspekhi*, **44**, 173-197. https://doi.org/10.1070/PU2001v044n02ABEH000760

[15] Sapozhnikov, K.V., Vetrov, V.V., Pulnev, S.A. and Kustov, S.B. (1996) Acoustic-Pseudoelastic Effect and Internal Friction during Stress-Induced Martensitic Transformation in Cu-Al-Ni Single Crystals. *Scripta Materialia*, **34**, 1543-1548. https://doi.org/10.1016/1359-6462(96)00013-9

[16] Goliboroda, I., Rusinko, K. and Tanaka, K. (1999) Description of a Fe-Based Shape

Memory Alloy Thermomechanical Behavior in Terms of the Synthetic model. *Computational materials science*, **13**, 218-226. https://doi.org/10.1016/S0927-0256(98)00092-5

[17] Rusinko, A. and Rusinko, K. (2011) Plasticity and Creep of Metals. Springer Science and Business Media, Heidelberg, 433. https://doi.org/10.1007/978-3-642-21213-0

[18] Rusynko, K.M. and Shandrivskyi, A.H. (1996) Irreversible Deformation in the Course of a Martensite Transformation. *Materials Science*, **31**, 786-789. https://doi.org/10.1007/BF00558603

[19] Likhachov, V.A. and Malinin, V.G. (1993) Structural-Analytic Theory of Elasticity. Nauka, St. Petersburg. (In Russian)